Research Paper
Computational Methods for Differential Equations
http://cmde.tabrizu.ac.ir
Vol. *, No. *, *, pp. 1-15
DOI:10.22034/cmde.2025.66426.3098

Investigating novel optical soliton solutions and qualitative analysis of the traveling waves for a Kolmogorov-Petrovsky-Piskunov equation

Derya Yıldırım Sucu[1], Seydi Battal Gazi Karakoc[1,*], Asit Saha[2], and Khalid K. Ali[3,4]

[1]Department of Mathematics, Faculty of Science and Art, Nevşehir Hacı Bektaş Veli University, Nevşehir, 50300, Türkiye.

[2]Department of Mathematics, Sikkim Manipal Institute of Technology, Sikkim Manipal University, Majitar, Sikkim 737136, India.

[3]Mathematics Education Program, Faculty of Education and Arts, Sohar University, Sohar 311, Oman.

[4]Department of Mathematics, Faculty of Science, AL-Azhar University. Nasr City, P.N.Box: 11884- Cairo, Egypt.

Abstract

The main target of this article is to obtain new and several analytical and numerical traveling wave solutions of the Kolmogorov- Petrovsky-Piskunov (KPP) equation. Furthermore qualitative analysis of the traveling waves for the equation is presented through phase plane analysis. The genetics model introduced the equation for the diffusion of a beneficial gene throughout a population. Subsequently, it was used with several chemical, biological, and physical models. To address the inherent complexities associated with the nonlinear equation, the authors employed highly effective techniques: Firstly $(\frac{\mathfrak{G}'}{\omega\mathfrak{G}'+\mathfrak{G}+r})$-expansion technique is implemented to create some alternative exact solutions of the equation. A strong and popular method for getting exact solutions of nonlinear partial differential equations (PDEs) is the $(\frac{\mathfrak{G}'}{\omega\mathfrak{G}'+\mathfrak{G}+r})$ method. Next, a collocation approach based on the septic B-spline approximation has been introduced and put into practice for the numerical solution of the equation taking various test problem parameter values into consideration. The appropriate solutions for two test problems are found by computing the L_2 and L_∞ error norms, which highlights the significance of the procedure and demonstrates its applicability and credibility. The numerical findings are inferred to match the analytical answers well, suggesting that the existing B-spline collocation algorithm is a strong and appealing algorithm. The results are tabulated and reported both modally and in terms of productivity of the procedure. Analytical and numerical results make the methods more convenient and systematically handle the nonlinear solution process. Qualitative analysis of the traveling waves for the Kolmogorov-Petrovsky-Piskunov Equation is presented through phase plane analysis. The results produced from both analytical and numerical methods demonstrate the great utility of this study for scientists tasked with identifying characteristics and features of nonlinear processes across a variety of scientific domains.

Keywords. Kolmogorov- Petrovsky-Piskunov, $(\frac{\mathfrak{G}'}{\omega\mathfrak{G}'+\mathfrak{G}+r})$-expansion technique, Finite element method, Collocation, Septic B-spline, Qualitative analysis.

2010 Mathematics Subject Classification. 65N30, 65D07, 74S05, 74J35, 76B25.

1. Introduction

It is common knowledge that nonlinear wave equations and their solutions have significant applications in many branches of fluid dynamics and mathematical physics. One of the most successful theories for the mathematical description of the propagation of species is based on the "traveling wave solutions" (TWSs). It has been discovered that many nonlinear partial differential equations (NLPDEs) have a variety of travelling wave solutions, making TWSs a significant form of solution. Following the well-known works by Fisher [9] and Kolmogorov, Petrovsky, and Piscunov [20] in 1937, there was a lot of interest in the topic of investigating TWSs for parabolic equations. This topic is

Received: 15 March 2025; Accepted: 15 December 2025.
∗ Corresponding author. Email:sbgkarakoc@nevsehir.edu.tr.

extremely rich and relevant to genetic theory. The KPP equation is one of the equations that has been extensively researched recently regarding TWSs. It is defined as follows:

$$\frac{\partial \Psi(x,t)}{\partial t} + \frac{\partial^2 \Psi(x,t)}{\partial x^2} + \alpha \Psi(x,t) + \beta \Psi(x,t)^2 + \gamma \Psi(x,t)^3 = 0, \tag{1.1}$$

where α, β and γ are real constants. Another importance of KPP equation, also known as Fisher-Kolmogorov-Petrovsky-Piskunov's equation (Fisher-KPP) or Fisher's equation, can be contemplated as one of the variety of the reaction- diffusion equations (RDEs) [4]. Moreover, it is one of the elementary semilinear RDEs owing to the inhomogeneous term that reclines in it. RDEs can be used to mathematically represent a wide range of phenomena, including neurology, synergy, foam drainage, crystal development, soil-moisture, population genetics, cellular ecology, reaction chemistry, heat transfer, combustion, fluid dynamics, and more [12]. This equation is employed to set out the process of gene wave propagation. Also the model is useful in the the propagation of nerve pulses, the evolution of the set of duffing oscillators, and so forth. The KPP equation includes a number of well-known nonlinear equations from mathematical physics; For example, $\alpha = -1$, $\beta = 0$, $\gamma = 1$ it converts to the Newell-Whitehead equation, for $\alpha = a, \beta = -(a+1), \gamma = 1$ it is known as FitzHugh-Nagumo equation and for $\alpha = -1$, $\beta = 1$, $\gamma = 0$ this equation is an exceptional case of Fisher equation [35]. To take out the TWSs of the KPP equation, scientists have, so far, established some approximate and analytical approaches. These methods encompass the discrimination algorithm [36], homotopy analysis method [11, 30], Chebyshev wavelet technique [21], first integral technique [6], modified extended tanh method and an average linear finite difference scheme [37], Cole-Hopf transformation and Backlund transformations [25], undetermined technique [40], generalized two-dimensional differential transform method (GT-DDT) technique [33], $(G^{'}/G)$- expansion method [8], Bäcklund transformation method [10, 14, 28], tanh method [19], Adomian method [1], numerical approaches [3] and as well a direct algebraic approach [23], modified simple equation approach [39], Miura transformation [5], analytical ansatz method [24], Hirota bilinear method [7] and so on.

We use the novel $(\frac{\mathfrak{G}'}{\omega\mathfrak{G}'+\mathfrak{G}+r})$-expansion technique to obtain analytical solutions [2, 13, 32]. This approach, which is regarded as a variant of the $(\frac{G'}{G})$ [27], can be used for conformable fractional derivatives, fractional differential equations expounded by Jumarie [18], and differential equations of integer order. Furthermore, $(\frac{\mathfrak{G}'}{\omega\mathfrak{G}'+\mathfrak{G}+r})-$ expansion method employed here can be viewed as a specific realization within the broader framework of the transformed rational function method which utilizes rational transformations of solutions to auxiliary ordinary differential equations to construct exact solutions for nonlinear PDEs [26]. Our approach leverages a specific auxiliary equation structure Eqs. (8) and (9) to systematically generate new solution families for the KPP equation. Like any other approach, it has drawbacks, especially when used on higher-order PDEs. If the equation cannot be readily reduced to an ODE or converted into a suitable form, using this method becomes challenging.

One of the best methods for solving partial differential equations (PDEs) is the finite element method. B-spline interpolation functions have gained popularity in approximation theory as a way to solve boundary-value problems. For numerical calculations, the previously described functions are quite helpful. The majority of integrals in numerical methods are zero, therefore spline functions can be both differentiable and integrable because they are piecewise polynomials. Because of its straightforward implementation and programmable calculating approach, the B-spline-based collocation method is an especially useful technology [15]. As such, it needs less computing work than other existing techniques. In addition, these methods, which are based on spline functions to obtain numerical solutions of differential equations, can turn into band matrices that can be easily solved with low-cost calculations and some algorithms in the market. However, as the system parameters change, analyzing the dynamic features of wave solutions of nonlinear evolution equations might reveal qualitative shifts in the system's genesis [16].

The $(\frac{\mathfrak{G}'}{\omega\mathfrak{G}'+\mathfrak{G}+r})$-expansion method employed here can be viewed as a specific realization within the broader framework of the transformed rational function method [26], which utilizes rational transformations of solutions to auxiliary ordinary differential equations to construct exact solutions for nonlinear PDEs. Our approach leverages a specific auxiliary equation structure to systematically generate new solution families for the KPP equation.

Although the KPP equation has received a lot of attention, finding more intriguing new traveling wave solutions continues to be a significant contribution. To add to the body of knowledge, novel exact and numerical solutions to the KPP problem are examined in this paper. Two highly effective techniques have been used to achieve our

goal: the finite element approach and the $(\frac{\mathfrak{G}'}{\omega\mathfrak{G}'+\mathfrak{G}+r})$-expansion method. Structure of the document is as follows: In Section 2, we start with the model's mathematical analysis. Section 3 examines the $(\frac{\mathfrak{G}'}{\omega\mathfrak{G}'+\mathfrak{G}+r})$-expansion approach strategy. In Section 4, $(\frac{\mathfrak{G}'}{\omega\mathfrak{G}'+\mathfrak{G}+r})$- expansion method is employed to acquire some new family of analytical solutions of the equation. Section 5 discusses the graphical representation of several of these solutions. The construction of the numerical method and its application to the equation are given in Section 6. Then in Section 7, in order to show the performance and sensitiveness of the method, the problem has been solved by taking different parameters and the results are shown in tables. In Section 8, qualitative analysis of the nonlinear TWSs of Eq. (1.1) is analyzed. A brief presentation of the results is given in last Section.

2. Mathematical examination of the method

The following transformation is applied in order to obtain the TWS for Eq. (1.1):

$$\Psi(x,t) = v(\zeta), \tag{2.1}$$

here

$$\zeta = \kappa x - \nu t, \tag{2.2}$$

and the speed of the traveling wave is represented by ν. Eqs. (2.1) and (2.2) allow us to rewrite Eq. (1.1) as follows:

$$\kappa^2 v''^2 + \gamma v(\zeta)^3 - \nu v'(\zeta) = 0. \tag{2.3}$$

3. The $(\frac{\mathfrak{G}'}{\omega\mathfrak{G}'+\mathfrak{G}+r})$-expansion approach's configuration

The following is how we can formulate the governing equation:

$$F(\Psi, \Psi_{xx}, \Psi_t, ...) = 0. \tag{3.1}$$

Eq. (3.1) presents a polynomial function F based on the function Ψ and its derivatives in space and time. We may use a traveling wave transformation (2.1) to translate this PDE into an ordinary differential equation:

$$H(v, v'', ...) = 0. \tag{3.2}$$

The $(\frac{\mathfrak{G}'}{\omega\mathfrak{G}'+\mathfrak{G}+r})$-expansion procedure involves the following crucial steps:

Step 1: Let's assume that the answer to (3.2) is as follows:

$$v(\zeta) = \sum_{i=0}^{N} s_i \Theta(\zeta)^i, \tag{3.3}$$

here $\Theta(\zeta) = (\frac{\mathfrak{G}'}{\omega\mathfrak{G}'+\mathfrak{G}+r})$, $\mathfrak{G}(\zeta)$ fulfill the second-order differential equation:

$$(\zeta)' - \frac{\mathfrak{S}}{\omega^2}\mathfrak{G}(\zeta) - \frac{\mathfrak{S}}{\omega^2}r, \tag{3.4}$$

where: s_i are unknown constants, $\mathfrak{S}$, $\mathcal{L}$, and ω are constants that will be found later. On the other hand $\Theta = \Theta(\zeta)$ satisfies the ODE

$$\Theta'(\zeta) = (\mathcal{L} - \mathfrak{S} - 1)\Theta(\zeta)^2 + \frac{1}{\omega}(2\mathfrak{S} - \mathcal{L})\Theta(\zeta) - \frac{1}{\omega^2}\mathfrak{S}. \tag{3.5}$$

Step 2: Applying the idea from the previous part to determine N.

Step 3: Two sets of (3.5) solutions are obtained:

Class 1: If $\mathfrak{J} = \mathcal{L}^2 - 4\mathfrak{S} > 0$,

$$\mathfrak{G} = -r + \mathfrak{P}_1 e^{\frac{1}{2\omega}(-\mathcal{L}-\sqrt{\mathfrak{J}})\zeta} + \mathfrak{P}_2 e^{\frac{1}{2\omega}(-\mathcal{L}+\sqrt{\mathfrak{J}})\zeta}, \tag{3.6}$$

$\mathfrak{P}_1$ and $\mathfrak{P}_2$ are arbitrary constants, the relationship must be confirmed.
$r^2+\mathfrak{P}_1^2+\mathfrak{P}_2^2\neq 0$, then

$$\Theta(\zeta)=\frac{\mathfrak{P}_1(\mathcal{L}+\sqrt{\mathfrak{J}})+\mathfrak{P}_2(\mathcal{L}-\mathfrak{J})e^{\frac{\sqrt{\mathfrak{J}}\zeta}{\omega}}}{\omega\mathfrak{P}_1(\mathcal{L}-2+\sqrt{\mathfrak{J}})+\omega\mathfrak{P}_2(\mathcal{L}-2-\mathfrak{J})e^{\frac{\sqrt{\mathfrak{J}}\zeta}{\omega}}},$$

$$\Theta(\zeta)= \tag{3.7}$$

$$\frac{[\mathcal{L}(\mathfrak{P}_2-\mathfrak{P}_1)-\sqrt{\mathfrak{J}}(\mathfrak{P}_2+\mathfrak{P}_1)]\sinh(\frac{\sqrt{\mathfrak{J}}\zeta}{2\omega})+[\mathcal{L}(\mathfrak{P}_2+\mathfrak{P}_1)-\sqrt{\mathfrak{J}}(\mathfrak{P}_2-\mathfrak{P}_1)]\cosh(\frac{\sqrt{\mathfrak{J}}\zeta}{2\omega})}{\omega[(\mathcal{L}-2)(\mathfrak{P}_2-\mathfrak{P}_1)-\sqrt{\mathfrak{J}}(\mathfrak{P}_2+\mathfrak{P}_1)]\sinh(\frac{\sqrt{\mathfrak{J}}\zeta}{2\omega})+\omega[(\mathcal{L}-2)(\mathfrak{P}_2+\mathfrak{P}_1)-\sqrt{\mathfrak{J}}(\mathfrak{P}_2-\mathfrak{P}_1)]\cosh(\frac{\sqrt{\mathcal{J}}\zeta}{2\omega})}.$$

$$\Theta(\zeta)=\begin{cases}\frac{\mathcal{L}-2\mathfrak{S}}{2\omega(\mathcal{L}-\mathfrak{S}-1)}-\frac{\sqrt{\mathfrak{J}}}{2\omega(\mathcal{L}-\mathfrak{S}-1)}\tanh(\frac{\sqrt{\mathfrak{J}}\zeta}{2\omega}), & (\mathcal{L}-2)(\mathfrak{P}_2-\mathfrak{P}_1)-\sqrt{\mathfrak{J}}(\mathfrak{P}_2+\mathfrak{P}_1)=0,\\ \frac{\mathcal{L}-2\mathfrak{S}}{2\omega(\mathcal{L}-\mathfrak{S}-1)}-\frac{\sqrt{\mathfrak{J}}}{2\omega(\mathcal{L}-\mathfrak{S}-1)}\coth(\frac{\sqrt{\mathfrak{J}}\zeta}{2\omega}), & (\mathcal{L}-2)(\mathfrak{P}_2+\mathfrak{P}_1)-\sqrt{\mathfrak{J}}(\mathfrak{P}_2-\mathfrak{P}_1)=0.\end{cases} \tag{3.8}$$

Class 2: If $\mathfrak{J}=\mathcal{L}^2-4\mathfrak{S}<0$,

$$\mathfrak{S}=-r+e^{\frac{-\mathcal{L}q}{2\omega}}(\mathfrak{P}_1\cos(\frac{\sqrt{-\mathfrak{J}}\zeta}{2\omega})+\mathfrak{P}_2\sin(\frac{\sqrt{-\mathfrak{J}}\zeta}{2\omega})), \tag{3.9}$$

$$\Theta(\zeta)=\frac{(\mathcal{L}\mathfrak{P}_1-\sqrt{-\mathfrak{J}}\mathfrak{P}_2)\cos(\frac{\sqrt{-\mathfrak{J}}\zeta}{2\omega})+(\mathcal{L}\mathfrak{P}_2+\sqrt{-\mathfrak{J}}\mathfrak{P}_1)\sin(\frac{\sqrt{-\mathfrak{J}}\zeta}{2\omega})}{\omega((\mathcal{L}-2)\mathfrak{P}_1-\sqrt{-\mathfrak{J}}\mathfrak{P}_2)\cos(\frac{\sqrt{-\mathfrak{J}}\zeta}{2\omega})+\omega((\mathcal{L}-2)\mathfrak{P}_2+\sqrt{-\mathfrak{J}}\mathfrak{P}_1)\sin(\frac{\sqrt{-\mathfrak{J}}\zeta}{2\omega})}. \tag{3.10}$$

$$\Theta(\zeta)=\begin{cases}\frac{\mathcal{L}-2\mathfrak{S}}{2\omega(\mathcal{L}-\mathfrak{S}-1)}+\frac{\sqrt{-\mathfrak{J}}}{2\omega(\mathcal{L}-\mathfrak{S}-1)}\tan(\frac{\sqrt{-\mathfrak{J}}\zeta}{2\omega}), & (\mathcal{L}-2)\mathfrak{P}_2+\sqrt{-\mathfrak{J}}\mathfrak{P}_1=0,\\ \frac{\mathcal{L}-2\mathfrak{S}}{2\omega(\mathcal{L}-\mathfrak{S}-1)}-\frac{\sqrt{-\mathfrak{J}}}{2\omega(\mathcal{L}-\mathfrak{S}-1)}\cot(\frac{\sqrt{-\mathfrak{J}}\zeta}{2\omega}), & (\mathcal{L}-2)\mathfrak{P}_1-\sqrt{-\mathfrak{J}}\mathfrak{P}_2=0.\end{cases} \tag{3.11}$$

Step 4: When (3.3) and (3.4) are added to (3.2), the coefficients with the same powers of $\Theta(\zeta)$ vanish, revealing a system of equations. To find the solution to this system, use the Mathematica software.

4. Mathematical solutions of the method

The $(\frac{\mathfrak{S}'}{\omega\mathfrak{S}'+\mathfrak{S}+r})$-expansion method is used in this section to infer the analytical solutions for the two different instances that are studied in Eq. (1.1). For nonlinear differential equations, the $(\frac{\mathfrak{S}'}{\omega\mathfrak{S}'+\mathfrak{S}+r})$- expansion method is a powerful analytical method that is used to approximate solutions with remarkable efficiency.

Integrating the idea of balance principle with (2.3) between the terms v'' and v^3 provides $N+2=3N$, which suggests that $N=1$.We describe the solution to (2.3) using (3.3) as follows:

$$v(\zeta)=\sum_{i=0}^{1}s_i\Theta(\zeta)^i. \tag{4.1}$$

Eq. (4.1) is substituted for Eq. (2.3) and the coefficients of like powers of $(\frac{\mathfrak{S}'}{\omega\mathfrak{S}'+\mathfrak{S}+r})$ are equated to zero to provide the following system:

$$\alpha s_0+\beta s_0^2+\gamma s_0^3+\frac{\kappa^2\mathcal{L}\mathfrak{S}s_1}{\omega^3}-\frac{2\kappa^2\mathfrak{S}^2s_1}{\omega^3}+\frac{\mathfrak{S}\nu s_1}{\omega^2}=0, \tag{4.2}$$

$$\alpha s_1+2\beta s_0s_1+3\gamma s_0^2s_1+\frac{\kappa^2\mathcal{L}^2s_1}{\omega^2}-\frac{6\kappa^2\mathcal{L}\mathfrak{S}s_1}{\omega^2}+\frac{6\kappa^2\mathfrak{S}^2s_1}{\omega^2}+\frac{2\kappa^2\mathfrak{S}s_1}{\omega^2}+\frac{\mathcal{L}\nu s_1}{\omega}-\frac{2\mathfrak{S}\nu s_1}{\omega}=0, \tag{4.3}$$

$$\beta s_1^2+3\gamma s_0s_1^2-\frac{3\kappa^2\mathcal{L}^2s_1}{\omega}+\frac{9\kappa^2\mathcal{L}\mathfrak{S}s_1}{\omega}+\frac{3\kappa^2\mathcal{L}s_1}{\omega}-\frac{6\kappa^2\mathfrak{S}^2s_1}{\omega}-\frac{6\kappa^2\mathfrak{S}s_1}{\omega}-\mathcal{L}\nu s_1+\mathfrak{S}\nu s_1+\nu s_1=0, \tag{4.4}$$

$$\gamma s_1^3+2\kappa^2\mathcal{L}^2s_1-4\kappa^2\mathcal{L}\mathfrak{S}s_1-4\kappa^2\mathcal{L}s_1+2\kappa^2\mathfrak{S}^2s_1+4\kappa^2\mathfrak{S}s_1+2\kappa^2s_1=0. \tag{4.5}$$

The aforementioned set of equations could be solved with the Mathematica program to generate the following sets of solutions:

Set 1:

$$s_0=\frac{\nu\left(\kappa^2(\mathcal{L}-2\mathfrak{S})+\nu\omega\right)}{\beta\kappa^2\omega},\quad s_1=\frac{2\nu(-\mathcal{L}+\mathfrak{S}+1)}{\beta},\quad \gamma=-\frac{\beta^2\kappa^2}{2\nu^2},\quad \alpha=\frac{\frac{\kappa^4\left(\mathcal{L}^2-4\mathfrak{S}\right)}{\omega^2}-\nu^2}{2\kappa^2}. \tag{4.6}$$

Set2:

$$\begin{aligned}
s_0&=\frac{3\kappa^2\left(\mathcal{L}\sqrt{\mathcal{L}^2-4\mathfrak{S}}-2\mathfrak{S}\left(\sqrt{\mathcal{L}^2-4\mathfrak{S}}+2\right)+\mathcal{L}^2\right)-\nu\omega\left(\sqrt{\mathcal{L}^2-4\mathfrak{S}}+\mathcal{L}-2\mathfrak{S}\right)}{2\beta\omega^2},\\
s_1&=\frac{(\mathcal{L}-\mathfrak{S}-1)\left(\nu\omega-3\kappa^2\sqrt{\mathcal{L}^2-4\mathfrak{S}}\right)}{\beta\omega},\quad \alpha=\frac{\nu\omega\sqrt{\mathcal{L}^2-4\mathfrak{S}}-\kappa^2\left(\mathcal{L}^2-4\mathfrak{S}\right)}{\omega^2},\\
\gamma&=-\frac{2\beta^2\kappa^2\omega^2}{9\kappa^4\left(\mathcal{L}^2-4\mathfrak{S}\right)-6\kappa^2\nu\omega\sqrt{\mathcal{L}^2-4\mathfrak{S}}+\nu^2\omega^2}.
\end{aligned} \tag{4.7}$$

Set3:

$$\begin{aligned}
s_0&=\frac{3\kappa^2\left(-\mathcal{L}\sqrt{\mathcal{L}^2-4\mathfrak{S}}+2\mathfrak{S}\left(\sqrt{\mathcal{L}^2-4\mathfrak{S}}-2\right)+\mathcal{L}^2\right)+\nu\omega\left(\sqrt{\mathcal{L}^2-4\mathfrak{S}}-\mathcal{L}+2\mathfrak{S}\right)}{2\beta\omega^2},\\
s_1&=\frac{(\mathcal{L}-\mathfrak{S}-1)\left(3\kappa^2\sqrt{\mathcal{L}^2-4\mathfrak{S}}+\nu\omega\right)}{\beta\omega},\quad \alpha=-\frac{\kappa^2\left(\mathcal{L}^2-4\mathfrak{S}\right)+\nu\omega\sqrt{\mathcal{L}^2-4\mathfrak{S}}}{\omega^2},\\
\gamma&=-\frac{2\beta^2\kappa^2\omega^2}{9\kappa^4\left(\mathcal{L}^2-4\mathfrak{S}\right)+6\kappa^2\nu\omega\sqrt{\mathcal{L}^2-4\mathfrak{S}}+\nu^2\omega^2}.
\end{aligned} \tag{4.8}$$

By plugging the values from Equations (4.6), (4.7) and (4.8) into Eq. (4.1) and utilizing Equations (3.7),(3.8), (3.10) and (3.11), we can determine $v(\zeta)$. We may then find $v(\zeta)$ by inserting $v(\zeta)$ into Eq. (3.3). Finally, we may find the solutions of Eq.(1.1) by substituting $v(\zeta)$ in Eq. (2.1) and Eq. (2.2):

Family 1: When $\mathfrak{J}=\mathcal{L}^2-4\mathfrak{S}>0$, solutions rely on the hyperbolic function:

$$\Psi_1(x,t)=\frac{\nu\left(\kappa^2(\mathcal{L}-2\mathfrak{S})+\nu\omega\right)}{\beta\kappa^2\omega}+\frac{2\nu(-\mathcal{L}+\mathfrak{S}+1)}{\beta}\Theta(\zeta), \tag{4.9}$$

$$\begin{aligned}
\Psi_2(x,t)=&\frac{3\kappa^2\left(\mathcal{L}\sqrt{\mathcal{L}^2-4\mathfrak{S}}-2\mathfrak{S}\left(\sqrt{\mathcal{L}^2-4\mathfrak{S}}+2\right)+\mathcal{L}^2\right)-\nu\omega\left(\sqrt{\mathcal{L}^2-4\mathfrak{S}}+\mathcal{L}-2\mathfrak{S}\right)}{2\beta\omega^2}\\
&+\frac{(\mathcal{L}-\mathfrak{S}-1)\left(\nu\omega-3\kappa^2\sqrt{\mathcal{L}^2-4\mathfrak{S}}\right)}{\beta\omega}\Theta(\zeta),
\end{aligned} \tag{4.10}$$

$$\begin{aligned}
\Psi_3(x,t)=&\frac{3\kappa^2\left(-\mathcal{L}\sqrt{\mathcal{L}^2-4\mathfrak{S}}+2\mathfrak{S}\left(\sqrt{\mathcal{L}^2-4\mathfrak{S}}-2\right)+\mathcal{L}^2\right)+\nu\omega\left(\sqrt{\mathcal{L}^2-4\mathfrak{S}}-\mathcal{L}+2\mathfrak{S}\right)}{2\beta\omega^2}\\
&+\frac{(\mathcal{L}-\mathfrak{S}-1)\left(3\kappa^2\sqrt{\mathcal{L}^2-4\mathfrak{S}}+\nu\omega\right)}{\beta\omega}\Theta(\zeta),
\end{aligned} \tag{4.11}$$

where

$$\Theta(\zeta)=\frac{[\mathcal{L}(\mathfrak{P}_2-\mathfrak{P}_1)-\sqrt{\mathfrak{J}}(\mathfrak{P}_2+\mathfrak{P}_1)]\sinh(\frac{\sqrt{\mathfrak{J}}\zeta}{2\omega})+[\mathcal{L}(\mathfrak{P}_2+\mathfrak{P}_1)-\sqrt{\mathfrak{J}}(\mathfrak{P}_2-\mathfrak{P}_1)]\cosh(\frac{\sqrt{\mathfrak{J}}\zeta}{2\omega})}{\omega[(\mathcal{L}-2)(\mathfrak{P}_2-\mathfrak{P}_1)-\sqrt{\mathfrak{J}}(\mathfrak{P}_2+\mathfrak{P}_1)]\sinh(\frac{\sqrt{\mathfrak{J}}\zeta}{2\omega})+\omega[(\mathcal{L}-2)(\mathfrak{P}_2+\mathfrak{P}_1)-\sqrt{\mathcal{J}}(\mathfrak{P}_2-\mathfrak{P}_1)]\cosh(\frac{\sqrt{\mathfrak{J}}\zeta}{2\omega})}, \tag{4.12}$$

$$\Theta(\zeta)=\begin{cases}\frac{\mathcal{L}-2\mathfrak{S}}{2\omega(\mathcal{L}-\mathfrak{S}-1)}-\frac{\sqrt{\mathfrak{J}}}{2\omega(\mathcal{L}-\mathfrak{S}-1)}\tanh(\frac{\sqrt{\mathfrak{J}}\zeta}{2\omega}), & (\mathcal{L}-2)(\mathfrak{P}_2-\mathfrak{P}_1)-\sqrt{\mathfrak{J}}(\mathfrak{P}_2+\mathfrak{P}_1)=0,\\ \frac{\mathcal{L}-2\mathfrak{S}}{2\omega(\mathcal{L}-\mathfrak{S}-1)}-\frac{\sqrt{\mathfrak{J}}}{2\omega(\mathcal{L}-\mathfrak{S}-1)}\coth(\frac{\sqrt{\mathfrak{J}}\zeta}{2\omega}), & (\mathcal{L}-2)(\mathfrak{P}_2+\mathfrak{P}_1)-\sqrt{\mathfrak{J}}(\mathfrak{P}_2-\mathfrak{P}_1)=0.\end{cases} \tag{4.13}$$

Family 2: When $\mathfrak{J}=\mathcal{L}^2-4\mathfrak{S}<0$, solutions rely on the trigonometric function:

$$\Psi_4(x,t)=\frac{\nu\left(\kappa^2(\mathcal{L}-2\mathfrak{S})+\nu\omega\right)}{\beta\kappa^2\omega}+\frac{2\nu(-\mathcal{L}+\mathfrak{S}+1)}{\beta}\Theta(\zeta), \tag{4.14}$$

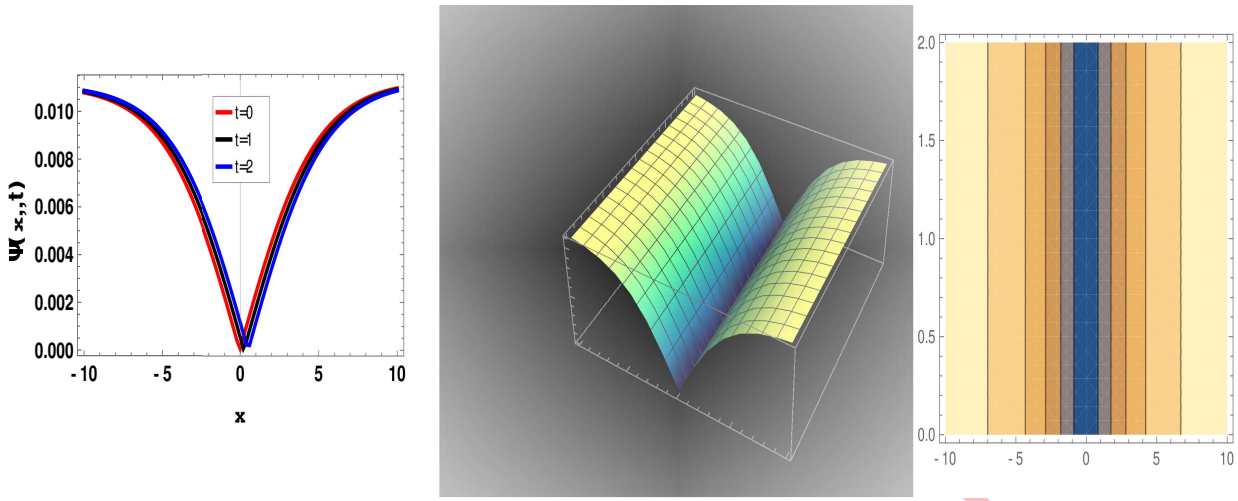

FIGURE 1. Graph of (4.9) with (4.13) and (4.6) at $\mathcal{L} = 0.1, \mathfrak{S} = 0.0001, \omega = 0.7, \kappa = 3, \nu = 0.008, \beta = 0.1$.

$$\Psi_5(x,t) = \frac{3\kappa^2\left(\mathcal{L}\sqrt{\mathcal{L}^2-4\mathfrak{S}} - 2\mathfrak{S}\left(\sqrt{\mathcal{L}^2-4\mathfrak{S}}+2\right)+\mathcal{L}^2\right) - \nu\omega\left(\sqrt{\mathcal{L}^2-4\mathfrak{S}}+\mathcal{L}-2\mathfrak{S}\right)}{2\beta\omega^2} + \frac{(\mathcal{L}-\mathfrak{S}-1)\left(\nu\omega - 3\kappa^2\sqrt{\mathcal{L}^2-4\mathfrak{S}}\right)}{\beta\omega}\Theta(\zeta), \tag{4.15}$$

$$\Psi_6(x,t) = \frac{3\kappa^2\left(-\mathcal{L}\sqrt{\mathcal{L}^2-4\mathfrak{S}} + 2\mathfrak{S}\left(\sqrt{\mathcal{L}^2-4\mathfrak{S}}-2\right)+\mathcal{L}^2\right) + \nu\omega\left(\sqrt{\mathcal{L}^2-4\mathfrak{S}}-\mathcal{L}+2\mathfrak{S}\right)}{2\beta\omega^2} + \frac{(\mathcal{L}-\mathfrak{S}-1)\left(3\kappa^2\sqrt{\mathcal{L}^2-4\mathfrak{S}} + \nu\omega\right)}{\beta\omega}\Theta(\zeta), \tag{4.16}$$

where

$$\Theta(\zeta) = \frac{(\mathcal{L}\mathfrak{P}_1 - \sqrt{-\mathfrak{J}}\mathfrak{P}_2)\cos(\frac{\sqrt{-\mathfrak{J}}\zeta}{2\omega}) + (\mathcal{L}\mathfrak{P}_2 + \sqrt{-\mathfrak{J}}\mathfrak{P}_1)\sin(\frac{\sqrt{-\mathfrak{J}}\zeta}{2\omega})}{\omega((\mathcal{L}-2)\mathfrak{P}_1 - \sqrt{-\mathfrak{J}}\mathfrak{P}_2)\cos(\frac{\sqrt{-\mathfrak{J}}\zeta}{2\omega}) + \omega((\mathcal{L}-2)\mathfrak{P}_2 + \sqrt{-\mathfrak{J}}\mathfrak{P}_1)\sin(\frac{\sqrt{-\mathfrak{J}}\zeta}{2\omega})}, \tag{4.17}$$

$$\Theta(\zeta) = \begin{cases} \frac{\mathcal{L}-2\mathfrak{S}}{2\omega(\mathcal{L}-\mathfrak{S}-1)} + \frac{\sqrt{-\mathfrak{J}}}{2\omega(\mathcal{L}-\mathfrak{S}-1)}\tan(\frac{\sqrt{-\mathfrak{J}}\zeta}{2\omega}), & (\mathcal{L}-2)\mathfrak{P}_2 + \sqrt{-\mathfrak{J}}\mathfrak{P}_1 = 0, \\ \frac{\mathcal{L}-2\mathfrak{S}}{2\omega(\mathcal{L}-\mathfrak{S}-1)} - \frac{\sqrt{-\mathfrak{J}}}{2\omega(\mathcal{L}-\mathfrak{S}-1)}\cot(\frac{\sqrt{-\mathfrak{J}}\zeta}{2\omega}), & (\mathcal{L}-2)\mathfrak{P}_1 - \sqrt{-\mathfrak{J}}\mathfrak{P}_2 = 0. \end{cases} \tag{4.18}$$

5. Visual Representations

In this paper, we examine the generated equations using a mix of analytical methods. Gaining a deeper understanding of the system and its operation is our primary goal. We include 2D and 3D figures that illustrate the analytical solution we discovered in order to clearly illustrate our conclusions. Visual representations of the solutions' behavior are provided by these figures, which also highlight the effects of different parameters and offer helpful insights into how the system develops under various circumstances. The analytical solutions for Eqs. (4.9) to (4.18) in Figures 1–5 are the main focus of our attention.

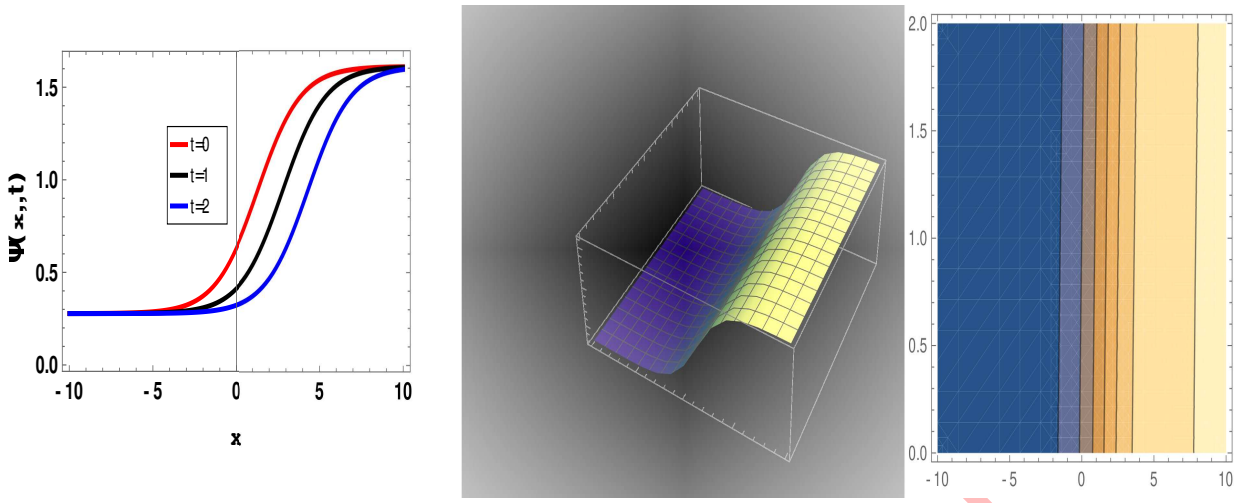

FIGURE 2. Graph of (4.10) with (4.12) and (4.7) at $\mathfrak{S} = 0.001, \mathcal{L} = 0.1, \mathfrak{P}_1 = 1.5, \mathfrak{P}_2 = 1, \omega = 0.3, \kappa = 2, \nu = 0.3, \beta = 3$.

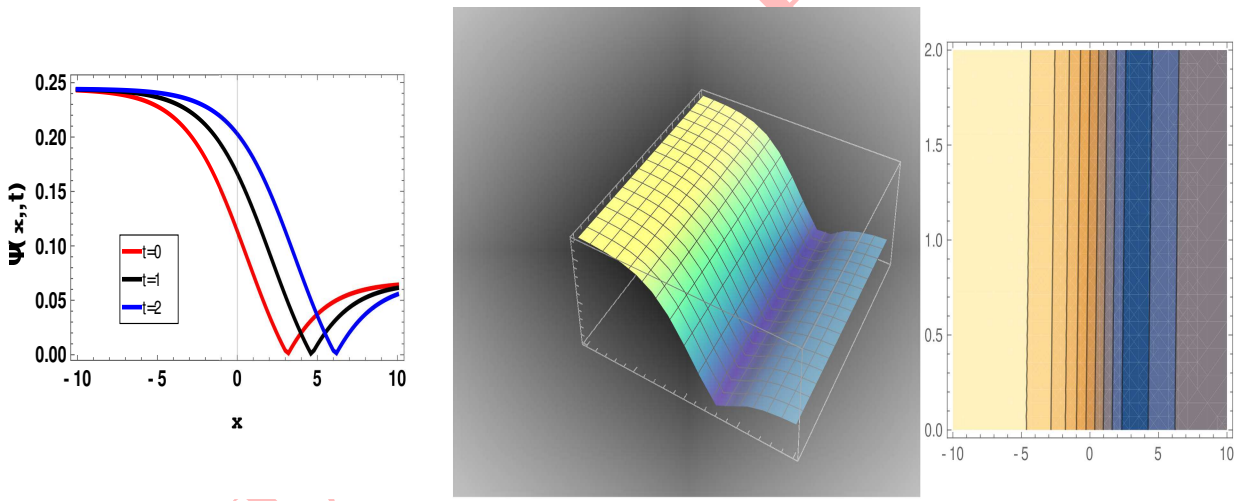

FIGURE 3. Graph of (4.11) with (4.12) and (4.8) at $\mathfrak{S} = 0.001, \mathcal{L} = 0.1, \mathfrak{P}_1 = 1.5, \mathfrak{P}_2 = 1, \omega = 0.3, \kappa = 2, \nu = 0.3, \beta = 3$.

6. Construction of the numerical method

In this section, we achieve the septic B-spline collocation finite element method to confirm and illustrate the accuracy and efficiency of the proposed method. Septic B-spline functions $\phi_m(x)$, $m = -3(3)N$, at the nodes x_m are defined over the solution interval $[x_L = a,\ x_R = b]$ in [29]. Because of their smoothness, local support, and capacity to manage local occurrences, B-spline functions are dependable tools for precisely and simply solving both linear and nonlinear partial differential equations. The emergence of a technique in the colocation procedure that only needs unknown parameters at certain nodes to construct the solution depends on the use of B-spline functions. Approximate solution

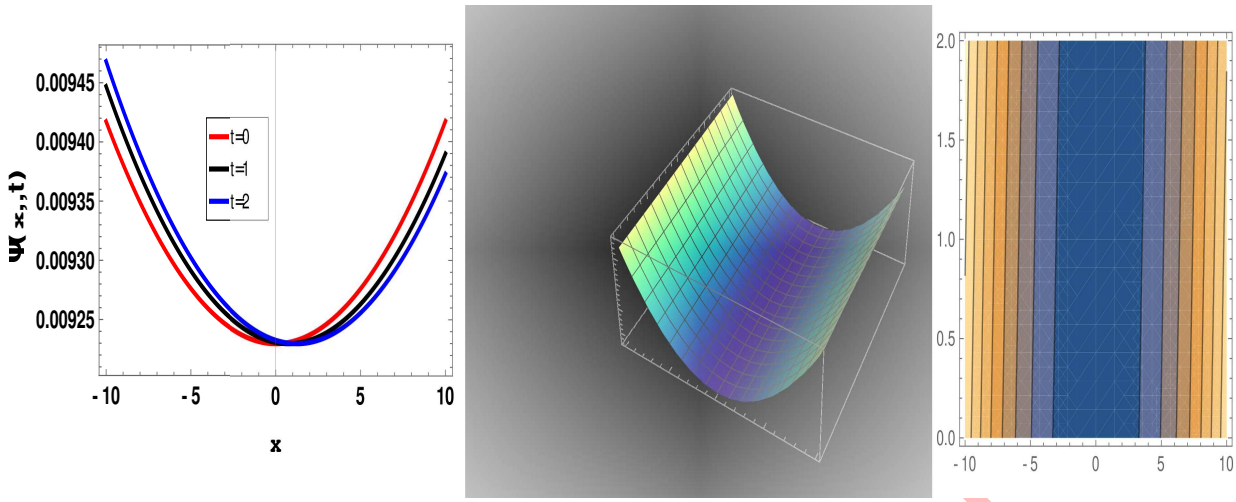

FIGURE 4. Graph of (4.15) with (4.18) and (4.7) at $\mathcal{L} = 0.001, \mathfrak{S} = 0.0001, \omega = 0.1, \kappa = 0.2, \nu = 0.05, \beta = 0.6$.

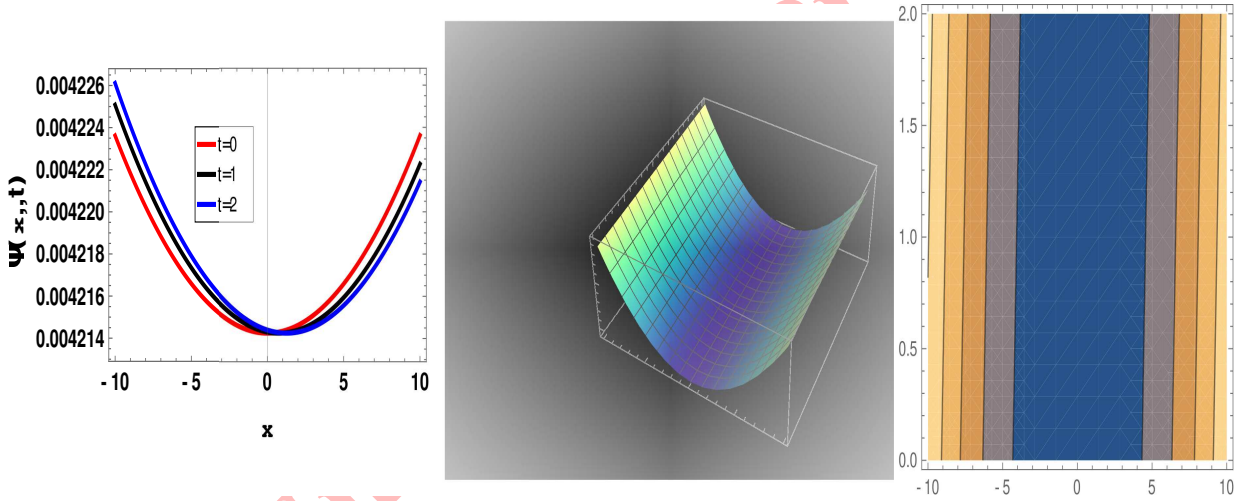

FIGURE 5. Graph of (4.16) with (4.18) and (4.8) at $\mathcal{L} = 0.001, \mathfrak{S} = 0.0001, \omega = 0.1, \kappa = 0.2, \nu = 0.05, \beta = 0.6$.

$u_{numeric}(x,t)$ for analytical solution $u_{exact}(x,t)$ can be given as a linear combination of septic B-splines as follows:

$$u_{numeric}(x,t) = \sum_{m=-3}^{N+3} \phi_m(x)\sigma_m(t). \tag{6.1}$$

Using the $h\xi = x - x_m$, $(0 \le \xi \le 1)$ transformation to the typical finite interval $[x_m, x_{m+1}]$ is planned to more easily practicable region $[0,1]$. Nodall values of u_m and its derivatives are deternined in terms of element parameters σ_m in the following form

$$u_{numeric}(x_m,t) = \sigma_{m-3} + 120\sigma_{m-2} + 1191\sigma_{m-1} + 2416\sigma_m + 1191\sigma_{m+1} + 120\sigma_{m+2} + \sigma_{m+3},$$

$$u'_m = \frac{7}{h}(-\sigma_{m-3} - 56\sigma_{m-2} - 245\sigma_{m-1} + 245\sigma_{m+1} + 56\sigma_{m+2} + \sigma_{m+3}),$$

$$u''_m = \frac{42}{h^2}(\sigma_{m-3} + 24\sigma_{m-2} + 15\sigma_{m-1} - 80\sigma_m + 15\sigma_{m+1} + 24\sigma_{m+2} + \sigma_{m+3}), \tag{6.2}$$
$$u'''_m = \frac{210}{h^3}(-\sigma_{m-3} - 8\sigma_{m-2} + 19\sigma_{m-1} - 19\sigma_{m+1} + 8\sigma_{m+2} + \sigma_{m+3}),$$
$$u^{iv}_m = \frac{840}{h^4}(\sigma_{m-3} - 9\sigma_{m-1} + 16\sigma_m - 9\sigma_{m+1} + \sigma_{m+3}),$$
$$u^{v}_m = \frac{2520}{h^5}(-\sigma_{m-3} + 4\sigma_{m-2} - 5\sigma_{m-1} + 5\sigma_{m+1} - 4\sigma_{m+2} + \sigma_{m+3}).$$

If the equalities (6.1) and (6.2) are used in the Eq.(1.1), following system of linearized ODEs are reached:

$$\begin{aligned}
&\dot{\sigma}_{m-3} + 120\dot{\sigma}_{m-2} + 1191\dot{\sigma}_{m-1} + 2416\dot{\sigma}_m + 1191\dot{\sigma}_{m+1} + 120\dot{\sigma}_{m+2} + \dot{\sigma}_{m+3} \\
&- \frac{42}{h^2}(\sigma_{m-3} + 24\sigma_{m-2} + 15\sigma_{m-1} - 80\sigma_m + 15\sigma_{m+1} + 24\sigma_{m+2} + \sigma_{m+3}) \\
&+ Z_{m1}\frac{7}{h}(-\sigma_{m-3} - 56\sigma_{m-2} - 245\sigma_{m-1} + 245\sigma_{m+1} + 56\sigma_{m+2} + \sigma_{m+3}) \\
&- Z_{m2}(\sigma_{m-3} + 120\sigma_{m-2} + 1191\sigma_{m-1} + 2416\sigma_m + 1191\sigma_{m+1} + 120\sigma_{m+2} + \sigma_{m+3}) = 0,
\end{aligned} \tag{6.3}$$

where $\dot{\sigma} = \frac{d\sigma}{dt}$ and

$$Z_{m1} = u^2,$$
$$Z_{m2} = u^3.$$

The system of ODEs (6.3) reduces to the following system of nonlinear equations when $\dot{\sigma}_i$ and σ_i are replaced by the forward difference approximation $\dot{\sigma}_i = \frac{\sigma_i^{n+1} - \sigma_i^n}{\Delta t}$ and Crank–Nicolson formulation $\sigma_i = \frac{\sigma_i^{n+1} + \sigma_i^n}{2}$, respectively:

$$\begin{aligned}
&\mathcal{L}_1\sigma^{n+1}_{m-3} + \mathcal{L}_2\sigma^{n+1}_{m-2} + \mathcal{L}_3\sigma^{n+1}_{m-1} + \mathcal{L}_4\sigma^{n+1}_{m} + \mathcal{L}_5\sigma^{n+1}_{m+1} + \mathcal{L}_6\sigma^{n+1}_{m+2} + \mathcal{L}_7\sigma^{n+1}_{m+3} \\
&= \mathcal{L}_7\sigma^{n}_{m-3} + \mathcal{L}_6\sigma^{n}_{m-2} + \mathcal{L}_5\sigma^{n}_{m-1} + \mathcal{L}_4\sigma^{n}_{m} + \mathcal{L}_3\sigma^{n}_{m+1} + \mathcal{L}_2\sigma^{n}_{m+2} + \mathcal{L}_1\sigma^{n}_{m+3},
\end{aligned} \tag{6.4}$$

where

$$\begin{aligned}
&\mathcal{L}_1 = [1 - E - KZ_{m1} - TZ_{m2}], && \mathcal{L}_2 = [120 - 24E - 56KZ_{m1} - 120TZ_{m2}], \\
&\mathcal{L}_3 = [1191 - 15E - 245KZ_{m1} - 1191TZ_{m2}], && \mathcal{L}_4 = [2416 + 80E - 2416TZ_{m2}], \\
&\mathcal{L}_5 = [1191 - 15E + 245KZ_{m1} - 1191TZ_{m2}], && \mathcal{L}_6 = [120 - 24E + 56KZ_{m1} - 120TZ_{m2}], \\
&\mathcal{L}_7 = [1 - E + KZ_{m1} - TZ_{m2}], &&
\end{aligned}$$
$$E = \frac{42}{h^2},\ K = \frac{7}{2h}\Delta t,\ T = \frac{1}{2}\Delta t,\ m = 0, 1, ..., N-1. \tag{6.5}$$

In order to acquire a distinctive solution of the system (6.4), six unknowns $\sigma_{-3}, \sigma_{-2}, \sigma_{-1}, \sigma_{N+1}, \sigma_{N+2}$, and σ_{N+3} must be eliminated.

7. Numerical simulations

We examine the KPP equation for a range of time and space division values in order to evaluate the effectiveness and validity of the suggested numerical approach. An exact wave feature of the KPP equation is

$$u(x,t) = [-\frac{1}{3} - \frac{\sqrt{8+12b}}{3} + \sqrt{-2b}\tanh(\sqrt{-b}(x - \frac{\sqrt{8+12b}}{3}t))], \tag{7.1}$$

under restriction $-8(1+6b)\sqrt{4+6b} - 11 = 0$ with the below initial and boundary conditions:

$$u(x,0) = [-\frac{1}{3} - \frac{\sqrt{8+12b}}{3} + \sqrt{-2b}\tanh(\sqrt{-b}x)], \tag{7.2}$$

where $b = -\frac{3}{16} - \frac{\sqrt{5}}{16}$.

In order to showcase the precision of our numerical approach, we have selected $[x_L = -70, x_R = 70]$ as the problem's interval and $t = 1$ as the processing's ultimate time, taking into account previous research findings. To verify our approach, we will employ the error norms that are commonly utilized in the literature, specifically L_2 and L_∞ [17, 38]:

$$L_2 = \|u_{exact} - u_{numeric}\|_2 \simeq \sqrt{h\sum_{j=1}^{N}\left|(u_{exact})_j - (u_{numeric})_j\right|^2}, \tag{7.3}$$

$$L_\infty = \|u_{exact} - u_{numeric}\|_\infty \simeq \max_j\left|(u_{exact})_j - (u_{numeric})_j\right|, \ j = 1, 2, ..., N. \tag{7.4}$$

In simulation calculations, typical values $\Delta t = 0.001$ with $h = 0.1, 0.01, 0.05$ and 0.005 were selected in order to agree with the literature. The results for the error norms L_2 and L_∞ computed over these values for step sizes and time levels are shown in Table 1. Consequently, it is simple to observe how the quantity of ranking points affects how the numerical approach behaves. Upon analyzing the table, it was discovered that the computed error norms L_2 and L_∞ were appropriately minimal. We can conclude that the numerical findings are positively impacted by increasing the number of time divisions. A $t = 0.05$ study was conducted on the approach. Secondly, Table 2 show some comparisons between recently acquired numerical results and various papers in the literature. It is evident from the table that the collocation approach in conjunction with the division methods performs better, quicker, and with greater reliability than the other approaches. The 3-dimensional example of descending bell-shaped wave features formed at chosen time intervals is evident when examining Figure 6 and 7. The wave's behavior, which involves sluggish motion and no form change, is depicted in the figures.

TABLE 1. The error norms for two values of h and Δt.

	$\Delta t = 0.001, h = 0.1$		$\Delta t = 0.001, h = 0.005$	
t	L_2	L_∞	L_2	L_∞
0.01	11.42×10^{-2}	18.06×10^{-3}	44.44×10^{-5}	80.55×10^{-5}
0.02	22.74×10^{-2}	35.94×10^{-3}	88.23×10^{-5}	14.16×10^{-4}
0.03	33.93×10^{-2}	53.64×10^{-3}	13.23×10^{-4}	20.39×10^{-4}
0.04	45.02×10^{-2}	71.17×10^{-3}	17.64×10^{-4}	26.99×10^{-4}
0.05	55.99×10^{-2}	88.52×10^{-7}	22.04×10^{-4}	33.50×10^{-4}
	$\Delta t = 0.001, h = 0.01$		$\Delta t = 0.001, h = 0.05$	
t	L_2	L_∞	L_2	L_∞
0.01	42.41×10^{-5}	69.35×10^{-5}	52.25×10^{-5}	80.55×10^{-5}
0.02	85.09×10^{-5}	13.69×10^{-4}	10.39×10^{-4}	14.16×10^{-4}
0.03	12.78×10^{-4}	20.39×10^{-4}	15.53×10^{-4}	20.39×10^{-4}
0.04	17.07×10^{-4}	26.99×10^{-4}	20.63×10^{-4}	26.99×10^{-4}
0.05	21.35×10^{-4}	33.50×10^{-4}	25.68×10^{-4}	33.50×10^{-4}

TABLE 2. The comparison of error norms for distinct values of h and Δt.

	$\Delta t = 0.001, h = 1/8$		$\Delta t = 0.001, h = 1/16$	
t	L_2	L_∞	L_2	L_∞
Ref. [37]	1.06456E-02	1.54297E-02	2.59637E-03	3.75879E-03
0.01	5.14640E-04	9.82253E-04	4.54164E-04	8.31462E-04
0.02	9.47241E-04	14.7435E-04	8.92579E-04	14.2336E-04
0.03	14.0282E-04	20.3937E-04	13.3645E-04	20.3934E-04
0.04	18.6252E-04	26.9953E-04	17.8104E-04	26.9951E-04
0.05	23.2164E-04	33.5007E-04	22.2512E-04	33.5005E-04

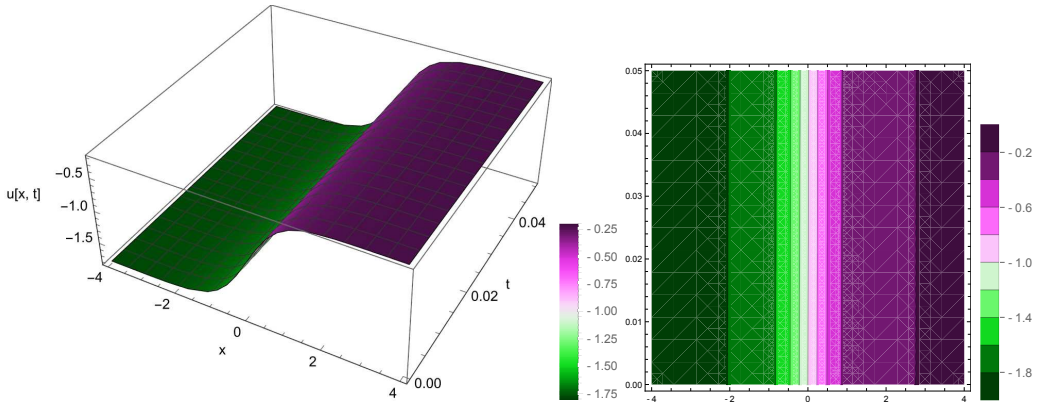

FIGURE 6. Numerical features of the problem for $\Delta t = 0.001$ and $h = 0.1$.

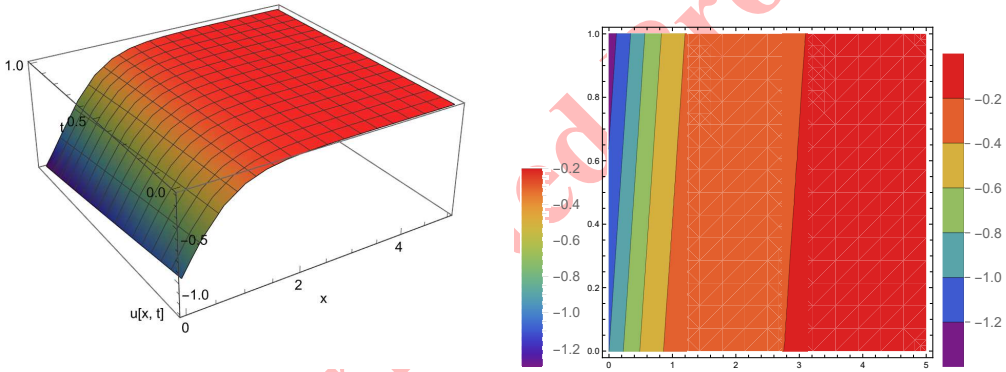

FIGURE 7. Numerical behaviours of the problem for $\Delta t = 0.01$ and $h = 0.1$.

8. Qualitative Analysis

We are interested to investigate te qualitative analysis of the nonlinear TWSs of Eq. (1.1). To explore all possible nonlinear TW of Eq. (1.1), one can employ a frame $\xi = x - vt$ with speed v. Then Eq. (1.1) becomes

$$-v\Psi_\xi + \Psi_{\xi\xi} + \alpha\Psi + \beta\Psi^2 + \gamma\Psi^3 = 0. \tag{8.1}$$

Then the system (8.1) is written as the following dynamical system (DS):

$$\begin{aligned} \psi_\xi &= P, \\ \mathfrak{P}_\xi &= vP - \alpha\Psi - \beta\Psi^2 - \gamma\Psi^3. \end{aligned} \tag{8.2}$$

The system (8.2) is a planar dynamical system [22, 31, 34] with α, β, γ and v as physical parameters. If $\beta^2 - 4\gamma\alpha > 0$, then the DS (8.2) has three equilibrium points at $E_0(\Psi_0, 0)$, $E_1(\Psi_1, 0)$, and $E_2(\Psi_2, 0)$, where $\Psi_0 = 0$, $\Psi_1 = \frac{-\beta+\sqrt{\beta^2-4\alpha\gamma}}{2\gamma}$ and $\Psi_2 = \frac{-\beta-\sqrt{\beta^2-4\alpha\gamma}}{2\gamma}$. If $\beta^2 - 4\gamma\alpha = 0$, then the DS (8.2) has two singular points or equilibrium points at $E_0(\Psi_0, 0)$ and $E_3(\Psi_3, 0)$, where $\Psi_3 = -\frac{\beta}{2\gamma}$. If $\beta^2 - 4\gamma\alpha < 0$, then the DS (8.2) has only one equilibrium point at $E_0(\Psi_0, 0)$. For each point $(\Psi_i, \mathfrak{P}_i)$ in the ΨP-plane, each trajectory or orbit in the phase portrait correlate with a traveling wave feature or solution of Eq. (1.1).

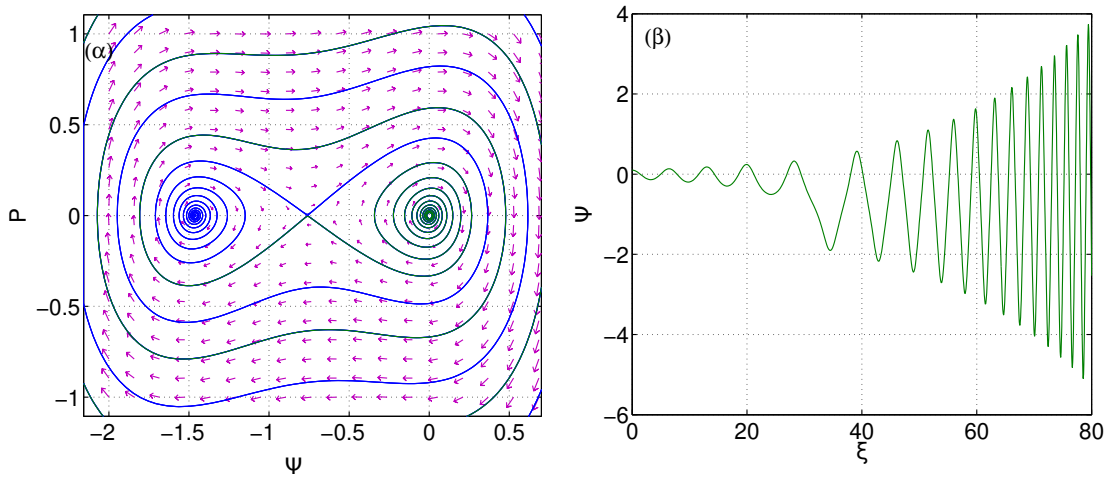

FIGURE 8. (left) Phase plot of the DS (8.2), (right) Plot of Ψ with respect to ξ for $v = 0.1,\ \alpha = 1,\ \beta = 2$, and $\gamma = 0.9$.

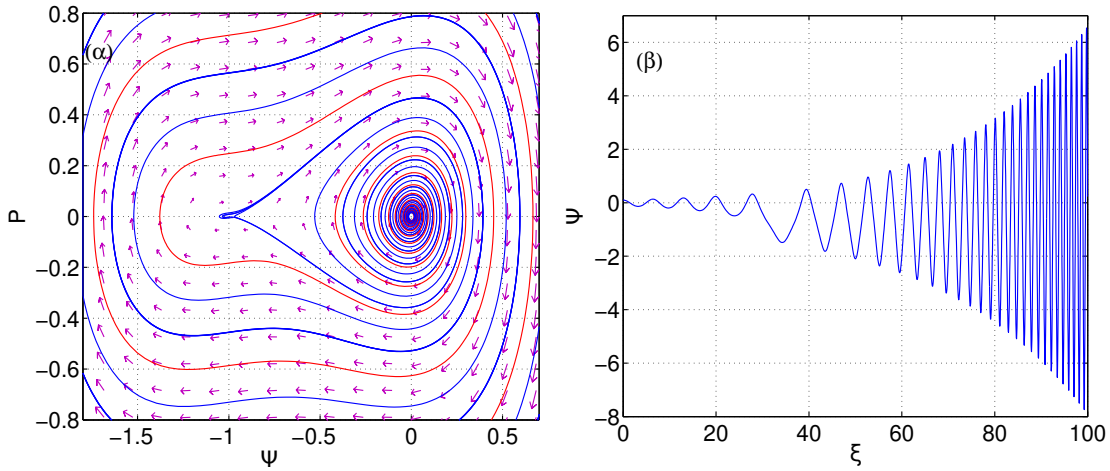

FIGURE 9. (left) Phase plot of the DS (8.2), (right) Plot of Ψ with respect to ξ for $v = 0.1,\ \alpha = 1,\ \beta = 2$, and $\gamma = 1$.

In Figure 8(a), phase plot of the DS (8.2) is presented for $v = 0.1,\ \alpha = 1,\ \beta = 2$, and $\gamma = 0.9$. It contains three singular or equilibrium points at $E_0(\Psi_0, 0)$, $E_1(\Psi_1, 0)$, and $E_2(\Psi_2, 0)$. There are two unstable spirals at $E_0(\Psi_0, 0)$ and $E_2(\Psi_2, 0)$. The unstable oscillation corresponding the unstable spiral at $E_0(\Psi_0, 0)$ is presented in Figure 8(b).

In Figure 9(a), phase plot of the DS (8.2) is presented for $v = 0.1,\ \alpha = 1,\ \beta = 2$, and $\gamma = 1$. It accommodates two singular or equilibrium points at $E_0(\Psi_0, 0)$ and $E_3(\Psi_3, 0)$. There is one unstable spiral at $E_0(\Psi_0, 0)$. The unstable oscillation corresponding the unstable spiral at $E_0(\Psi_0, 0)$ is presented in Figure 9(b).

In Figure 10(a), phase plot of the DS (8.2) is presented for $v = 0.1,\ \alpha = 1,\ \beta = 2$, and $\gamma = 1.1$. It contains only one equilibrium point at $E_0(\Psi_0, 0)$. There is only one unstable spiral at $E_0(\Psi_0, 0)$. The unstable oscillation corresponding the unstable spiral at $E_0(\Psi_0, 0)$ is presented in Figure 10(b).

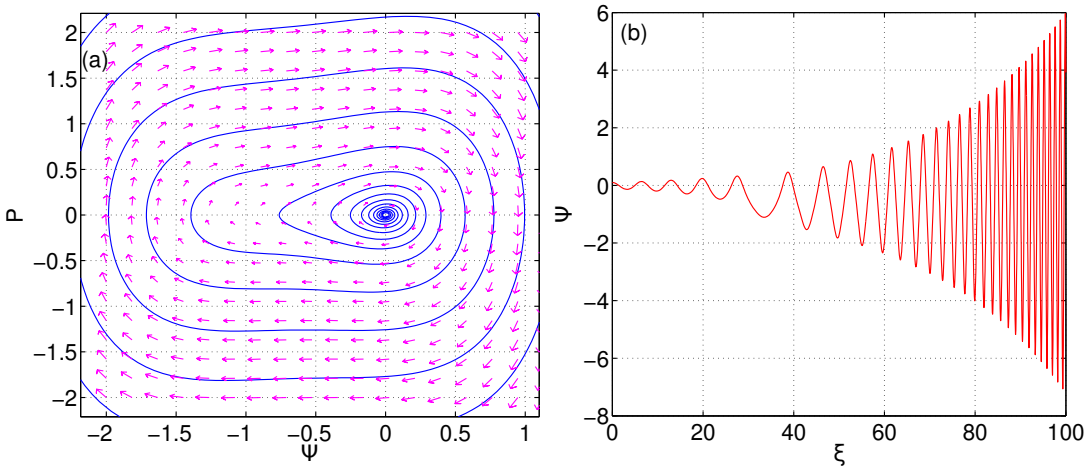

FIGURE 10. (left) Phase plot of the DS (8.2), (right) Plot of Ψ with respect to ξ for $v = 0.1$, $\alpha = 1$, $\beta = 2$, and $\gamma = 1.1$.

9. Conclusion

The implications of our research are twofold: Firstly, $(\frac{\mathfrak{G}'}{\omega\mathfrak{G}'+\mathfrak{G}+r})$-expansion method has been used for obtaining the exact solutions of the KPP equation. Since the method offers a wide range of exact wave solutions for a sizable class of nonlinear evolution equations, the applied method is a novel scheme that is also incredibly strong and effective. Secondly, the septic B-spline collocation method has been presented and implemented for the numerical solutions of the equation. For the purpose of numerical experiments, our method has been applied for the single solitary wave in which the exact solution is known. To assess the performance and validness of numerical algorithm L_2 and L_∞ error norms have been measured. For the sake of better understanding of the obtained solutions, some graphical illustrations are presented also for the two methods. Numerical experiments demonstrated that the results are obtained from the proposed method are efficient, reliable, fruitful, and powerful. The study's greatest feature is how well the two strategies for obtaining precise and quantifiable results were implemented. Qualitative analysis of the traveling wave features for the KPP equation is presented through phase plane analysis. All possible phase portraits with unstable spirals are depicted. The oscillatory wave solutions are presented corresponding to the unstable spirals. It is therefore possible to analyze NLPDEs, which frequently occur in engineering sciences, mathematical physics, and other scientific subjects, more successfully by using this straightforward yet effective method.

Acknowledgment

Asit Saha is thankful to Sikkim Manipal Institute of technology for the research support (6100/SMIT/R&D/Project/06/2022)

References

[1] G. Adomian, *The generalized Kolmogorov-Petrovskii-Piskunov equation*, Foundation of Pyhsics Letters, *8* (1995), 99-101.

[2] K. K. Ali, S. A. Al Qahtani, M. S. Mehanna, and A. M. Wazwaz, *Novel Soliton Solutions for the (3+1)-Dimensional Sakovich Equation Using Different Analytical techniques*, Hindawi, Journal of Mathematics, *2023* (2023), 4864334.

[3] J. R. Branco, J. A. Ferreira, and P. Oliveira, *Numerical methods for the generalized Fisher–Kolmogorov–Petrovskii–Piskunov equation*, Applied Numerical Mathematics, *57* (2007), 89-102.

[4] J. Canosa, *On a nonlinear diffusion equation describing population growth*, IBM Journal of Research and Development, *17*(4) (1973), 307–313.

[5] L. Cheng, Y. Zhang, and W. X. Ma, *An extended (2+1)-dimensional modified Korteweg–de Vries–Calogero–Bogoyavlenskii–Schiff equation*, Communications in Theoretical Physics, *77*(3) (2025), 035002.

[6] Y. M. Chu, S. Javeed, D. Baleanu, S. Riaz, and H. Rezazadeh, *New exact solutions of Kolmogorov Petrovskii Piskunov equation, Fitzhugh Nagumo equation, and Newell-Whitehead equation*, Advances in Mathematical Physics, *2020* (2020), 1-14.

[7] J. Chu, Y. Liu, and W. X. Ma, *Integrability and multiple-rogue and multi-soliton wave solutions of the (3+1)-dimensional Hirota–Satsuma–Ito equation,* Modern Physics Letters B, *39* (2025), 2550060.

[8] J. Feng, W. Li, and Q. Wan, *Using* $(G^{'}/G)$*-expansion method to seek the travelling wave solution of Kolmogorov-Petrovskii-Piskunov equation*, Applied Mathematics and Computation, *217* (2011), 5860–5865.

[9] R. A. Fisher, *The wave of advance of advantageous genes*, Annals of Eugenics, *7* (1937), 355–369.

[10] D. Gao, W. X. Ma, and X. Lü, *Wronskian solution, Bäcklund transformation and Painlevé analysis to a (2 + 1)-dimensional Konopelchenko–Dubrovsky equation*, Zeitschrift für Naturforschung A, *79*(9) (2024), 887–895.

[11] G. Hariharan, *The homotopy analysis method applied to the Kolmogorov–Petrovskii–Piskunov (KPP) and fractional KPP equations*, Journal of Mathematical Chemistry, *51*(3) (2013), 992-1000.

[12] T. Harko and M. K. Mak, *Exact travelling wave solutions of non-linear reaction-convection-diffusion equations-an Abel equation-based approach*, Journal of Mathematical Physics, *56*(11) (2015), 111501.

[13] B. Hong, *Assorted exact explicit solutions for the generalized Atangana's fractional BBM-Burgers equation with the dissipative term*, Frontiers in Physics, *10* (2022), 1-12.

[14] W. P. Hong and Y. D. Jung, *Auto-Bäcklund transformation and analytic solutions for general variable-coefficient KdV equation*, Physics Letters A, *257*(3-4) (1999), 149–152.

[15] S. B. G. Karakoc, D. Y. Sucu, and M. A. Taghachi, *Numerical simulation of genaralized Oskolkov eqaution via the septic B-spline Collocation method*, Journal of Universal Mathematics, *5*(2) (2022), 108-116.

[16] S. B. G. Karakoc, A. Saha, S. K. Bhowmik, and D. Y. Sucu, *Numerical and dynamical behaviors of nonlinear traveling wave solutions of the Kudryashov–Sinelshchikov equation*, Wave Motion, *118* (2023), 103121.

[17] S. B. G. Karakoc, K. Omrani, and D. Y. Sucu, *Numerical investigations of shallow water waves via Generalized Equal Width GEW Equation*, Applied Numerical Mathematics, *162* (2021), 249–264.

[18] L. Kaur and A. M. Wazwaz, *Dynamical analysis of soliton solutions for space-time fractional Calogero-Degasperis and Sharma-Tasso-Olver Equations*, Romanian Reports in Physics, *74* (2022), 1-17.

[19] A. H. Khater, W. Malfliet, D. K. Callebaut, and E. S. Kamel, *The tanh method, a simple transformation and exact analytical solutions for nonlinear reaction–diffusion equations*, Chaos, Solitons & Fractals, *14*(3) (2002), 513-522.

[20] A. Kolmogorov, I. Petrovsky, and N. Piscunov, *Etude de l'equation de la diffusion avec croissance de la quantité de matiere et son application a un probleme biologique*, Moscow University Mathematics Bulletin, *1* (1937), 1–25.

[21] T. Korkiatsakul, S. Koonprasert, and K. Neamprem, *New analytical solutions for time-fractional Kolmogorov–Petrovsky–Piskunov equation with variety of initial boundary conditions*, Mathematics, *7*(9) (2019), 1-20.

[22] G. C. Layek, *An Introduction to Dynamical Systems and Chaos*, Springer, New York, 2015.

[23] C. Liu, *The relation between the kink-type solution and the kink-bell-type solution of non-linear evolution equations*, Physics Letters A, *312* (2003), 41-48.

[24] W.X. Ma, *Lump waves and their dynamics of a spatial symmetric generalized KP model*, Romanian Reports in Physics, *76* (2024), 1-11.

[25] W. Ma and B. Fuchssteiner, *Explicit and exact solutions to a Kolmogorov-Petrovskii-Piskunov equation*, The International Journal of Non-Linear Mechanics, *31* (1995), 329–338.

[26] W. X. Ma and J. H. Lee, *A transformed rational function method and exact solutions to the 3+1 dimensional Jimbo–Miwa equation*, Chaos, Solitons & Fractals, *42*(3) (2009), 1356-1363.

[27] M. Niwas and S. Kumar, *Multi-peakons, lumps, and other solitons solutions for the (2+1)-dimensional generalized Benjamin-Ono equation: an inverse (G'/G)-expansion method and real-world applications*, Nonlinear Dynamics, *111* (2023), 22499–22512.

[28] A. Öğün and C. Kart, *Exact Solutions of Fisher and Generalized Fisher Equations with Variable Coefficients*, Acta Mathematicae Applicatae Sinica, English Series, *23*(4) (2007), 563-568.
[29] P. M. Prenter, *Splines and Variational Methods*, Wiley-interscience publication, New York, 1975.
[30] H. Rouhparvar, *Travelling wave solution of the Kolmogorov-Petrovskii-Piskunov equation by the first integral method*, Bulletin of the Malaysian Mathematical Sciences Society, *37*(1) (2014), 181-190.
[31] A. Saha and S. Banerjee, *Dynamical Systems and Nonlinear Waves in Plasmas*, CRC Press, 2021.
[32] M. Shakeel, N. A. Shah, and J. D. Chung , *Novel Analytical Technique to Find Closed Form Solutions of Time Fractional Partial Differential Equations*, Fractal and Fractional, *6* (2022), 1-22.
[33] L. Song and W. Wang, *Approximate solutions of nonlinear fractional Kolmogorov-Petrovskii-Piskunov equations using an enhanced algorithm of the generalized two-dimensional differential transform method,* Communications in Theoretical Physics, *58* (2012), 182–188.
[34] S. H. Strogatz, *Nonlinear Dynamics and Chaos With Applications to Physics*, Biology, Chemistry and Engineering, CRC Press, 2015.
[35] A. Ö. Ünal, *On the Kolmogorov-Petrovsky-Piskunov Equation*, Communications Faculty of Sciences University of Ankara Series A1 Mathematics and Statistics, *62*(1) (2013), 1–10.
[36] D. S. Wang and H. B. Li, *Single and multi-solitary wave solutions to a class of nonlinear evolution equations*, Journal of Mathematical Analysis and Applications, *343*(1) (2008), 273–298.
[37] B. Wongsaijai, T. Aydemir, T. Ak and S. Dhawan, *Analytical and numerical techniques for initial-boundary value problems of Kolmogorov–Petrovsky–Piskunov equation*, Numerical Methods for Partial Differential Equations, *40*(1) (2024), 1–18.
[38] W. Wu, J. Manafian, K. K. Ali, S. B. G. Karakoc, A. H. Taqi, and M. A. Mahmoud, *Numerical and analytical results of the 1D BBM equation and 2D coupled BBM-system by finite element method*, International Journal of Modern Physics B, *36*(28) (2022), 2250201.
[39] E. M. E. Zayed and S. H. Ibrahim, *Exact solutions of Kolmogorov-Petrovskii-Piskunov equation using the modified simple equation method*, Acta Mathematicae Applicatae Sinica, English Series, *30*(3) (2014), 749-754.
[40] W. G. Zhang, X. K. Hu, and X. Q. Ling, *Approximate analytical solution of the generalized Kolmogorov-Petrovsky-Piskunov equation with cubic nonlinearity*, Acta Mathematicae Applicatae Sinica, English Series, *39* (2023), 424–449.